Evidence for a Radical Relay Mechanism during Reaction of Surface-Immobilized Molecules

A. C. Buchanan, III,* Phillip F. Britt, Kimberly B. Thomas, and Cheryl A. Biggs

Contribution from the Chemical and Analytical Sciences Division, Oak Ridge National Laboratory, P.O. Box 2008, Oak Ridge, Tennessee 37831-6197

Received October 23, 1995[⊗]

Abstract: The impact of restricted mass transport on high-temperature, free-radical reactions has been explored through the use of organic compounds immobilized on silica surfaces by a thermally robust Si−O−$C_{aromatic}$ linkage. The rate of thermolysis of surface-immobilized 1,3-diphenylpropane (≈DPP) at 375 °C under vacuum, by a free-radical chain pathway, was found to be very sensitive (factor of 40 variation) to the structure and orientation of a second, neighboring spacer molecule on the surface. Compared with the inert aromatic spacers, (e.g. biphenyl) it was found that spacer molecules containing reactive benzylic C−H bonds (e.g. diphenylmethane) are capable of accelerating the ≈DPP thermolysis by a process that is unique to diffusionally constrained systems. A mechanism involving rapid serial hydrogen transfer steps on the surface is proposed, which results in radical intermediates being relayed across the surface and, hence, overcoming classical diffusional limitations.

Introduction

Organic radical chemistry continues to receive wide-spread attention in studies ranging from the development of kinetic clocks for probing chemical and biochemical transformations[1] to the development of new synthetic methods.[2] There has also been considerable general interest in organic chemical reactions performed in constrained media as typified by micelles, liquid crystals, zeolites, and clays, or on the surface of silica gels.[3] In fuel chemistry, the conversion of energy resources such as coal, oil shale, lignin, and biomass into liquid fuels or higher value chemicals generally involves some form of thermochemical processing.[4] As a consequence, organic radical reactions play a key role in governing the conversion efficiency and product quality for these processes. These geopolymers and biopolymers possess a complex, macromolecular structure that is often highly cross-linked.[5] As a consequence, in the early stages of thermochemical processing where most of the network structure is retained, many organic radical intermediates will experience diffusional constraints in their reactions. To gain a fundamental understanding of the potential impact of restricted mass transport on free radical reaction pathways relevant to fuel processing, the challenge is to design constrained model systems that can be investigated at temperatures of ca. 300−450 °C. The organic compounds investigated are then chosen to represent related structural features believed to be present in the macromolecules.

Several years ago we developed a method for covalently anchoring organic compounds to a silica surface.[6] The general methodology involves the condensation of a phenol with the surface hydroxyl groups of a high purity, nonporous, fumed silica.

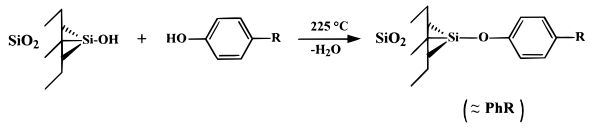

The resulting Si−O−C_{aryl} linkage to the surface has been shown to be thermally stable up to ca. 450 °C.[6,7] However, the linkage is readily cleaved in aqueous base such that surface-attached thermolysis products can be recovered for analysis. It has also been shown that residual underivatized surface silanols will not induce acid-catalyzed reactions for alkylbenzene substrates.[8] This permits the investigation of high temperature organic reactions involving free-radical intermediates under conditions of restricted diffusion. We have previously studied the thermolysis of surface-immobilized 1,2-diphenylethane, 1,3-diphenylpropane, and 1,4-diphenylbutane and have found that surface immobilization can have significant effects on thermal decomposition reaction rates and product selectivities compared with corresponding behavior in liquid or vapor phases.[6,9] Recently, we began designing silica surfaces containing two different components to probe the impact of the structure of neighboring molecules on the thermal decomposition of a given model compound.[10]

In this study, we examine the thermolysis of silica-immobilized 1,3-diphenylpropane (≈$Ph(CH_2)_3Ph$, or ≈DPP, where

[⊗] Abstract published in *Advance ACS Abstracts,* February 15, 1996.

(1) Leading references: (a) Newcomb, M. *Tetrahedron* **1993**, *49*, 1151 and references therein. (b) Beckwith, A. J.; Bowry, V. W. *J. Am. Chem. Soc.* **1994**, *116*, 2710.

(2) Leading references: (a) Jasperse, C. P.; Curran, D. P.; Fevig, T. L. *Chem. Rev.* **1991**, *91*, 1237. (b) Curran, D. P.; Shen, W. *J. Am. Chem. Soc.* **1993**, *115*, 6051. (c) Tanner, D. D., Ed. *Advances in Free Radical Chemistry*; JAI: London, 1990.

(3) Leading references: (a) Ramamurthy, V., Ed. *Photochemistry in Organized and Constrained Media*; VCH: New York, 1991. (b) Lem, G.; Kaprinidis, N. A.; Schuster, D. I.; Ghatlia, N. D.; Turro, N. J. *J. Am. Chem. Soc.* **1993**, *115*, 7009. (c) Laszlo, P. *Acc. Chem. Res.* **1986**, *19*, 121.

(4) (a) Gavalas, G. R. *Coal Pyrolysis*; Elsevier: Amsterdam, 1982. (b) Schlosberg, R. H. *Chemistry of Coal Conversion*; Plenum: New York, 1985. (c) Bridgwater, A. V., Ed. *Thermochemical Processing of Biomass*; Butterworths: London, 1984.

(5) (a) Green, T.; Kovac, J.; Brenner, D.; Larsen, J. W. In *Coal Structure*; Meyers, R. A., Ed.; Academic Press: NewYork, 1982; Chapter 6. (b) Berkowitz, N. *The Chemistry of Coal*; Elsevier: New York, 1985; Chapter 14. (c) Faulon, J.-L.; Hatcher, P. G. *Energy Fuels* **1994**, *8*, 402.

(6) Buchanan, A. C., III; Dunstan, T. D. J.; Douglas, E. C.; Poutsma, M. L. *J. Am. Chem. Soc.* **1986**, *108*, 7703.

(7) Mitchell, S. C.; Lafferty, C. J.; Garcia, R.; Snape, C. E.; Buchanan, A. C., III; Britt, P. F.; Klavetter, E. *Energy Fuels* **1993**, *7*, 331.

(8) Buchanan, A. C., III; Britt, P. F.; Thomas, K. B.; Biggs, C. A. *Energy Fuels* **1993**, *7*, 373.

(9) (a) Buchanan, A. C., III; Biggs, C. A. *J. Org. Chem.* **1989**, *54*, 517. (b) Britt, P. F.; Buchanan, A. C., III; *J. Org. Chem.* **1991**, *56*, 6132. (c) Britt, P. F.; Buchanan, A. C., III; Malcolm, E. A.; Biggs, C. A. *J. Anal. Appl. Pyrolysis* **1993**, *25*, 407.

(10) Buchanan, A. C., III; Britt, P. F.; Biggs, C. A. *Energy Fuels* **1990**, *4*, 415.

0002-7863/96/1518-2182$12.00/0 © 1996 American Chemical Society

the "≈" is used as a shorthand notation to represent a silica-immobilized compound) in the presence of a variety of coattached spacer molecules. DPP was chosen as the thermally reactive component, since it can be considered prototypical of linkages in coals that do not possess thermodynamically weak bonds easily cleaved at coal liquefaction temperatures (ca. 400 °C), but which nonetheless crack at measurable rates by radical chain processes. Thermolysis of DPP produces toluene and styrene as the principal products, and the chain propagation steps are shown in eqs 1 and 2. This radical chain decomposition

$$PhCH_2^{\bullet} + PhCH_2CH_2CH_2Ph \rightarrow PhCH_3 + PhCH^{\bullet}CH_2CH_2Ph \quad (1)$$

$$PhCH^{\bullet}CH_2CH_2Ph \rightarrow PhCH{=}CH_2 + PhCH_2^{\bullet} \quad (2)$$

process is observable for both fluid-phase[11] and silica-immobilized DPP[9a] at 375 °C, and the decomposition rate is governed by the rate of hydrogen atom transfer to form the 1,3-diphenyl-1-propyl radical (eq 1), which then undergoes facile unimolecular β-scission (eq 2). In the silica-immobilized case, the rate of hydrogen transfer between radicals and neighboring molecules on the surface should be highly dependent on the structure and proximity of these molecules. In a preliminary study of the thermolysis of ≈DPP in the presence of coattached biphenyl (≈BP) or diphenylmethane (≈DPM), we observed that the rate of ≈DPP thermolysis was substantially faster in the ≈DPM case.[10] We have now conducted a detailed investigation of this reaction, including isotopic labeling studies, to understand the origin of the rate enhancement. In addition, we present results from a systematic investigation of the effect of molecular structure of the spacer molecules on the radical decay pathway. The results lead us to propose the involvement of a novel hydrogen transfer, radical relay mechanism that is unique to diffusionally constrained environments.

Results

Preparation of Surface-Attached Substrates. The two-component surfaces were prepared by coattachment of phenolic precursors in a single step in an analogous manner to that described previously for 1,3-diphenylpropane,[9a] and as illustrated below for the case of 1,3-diphenylpropane and naphthalene. The

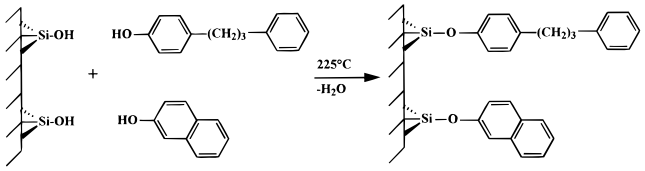

silica-immobilized substrates synthesized are shown in Figure 1, and the surface coverages and purities are given in Table 1. The silica employed in this work is a nonporous, amorphous, fumed silica with a surface area of 200 ± 25 $m^2\ g^{-1}$ and ca. 4.5 SiOH nm^{-2}. The stoichiometries were adjusted to prepare surfaces at saturation coverage, and to limit the ≈DPP surface coverage to 0.10−0.16 mmol g^{-1} with the balance of the available surface area (0.3−0.5 mmol g^{-1}, depending on spacer structure) covered by the spacer molecules. This permits a direct comparison of the thermolysis chemistry for ≈DPP as a function of spacer structure as well as with similar low surface coverages of ≈DPP alone. The reactions of the spacer phenols and the

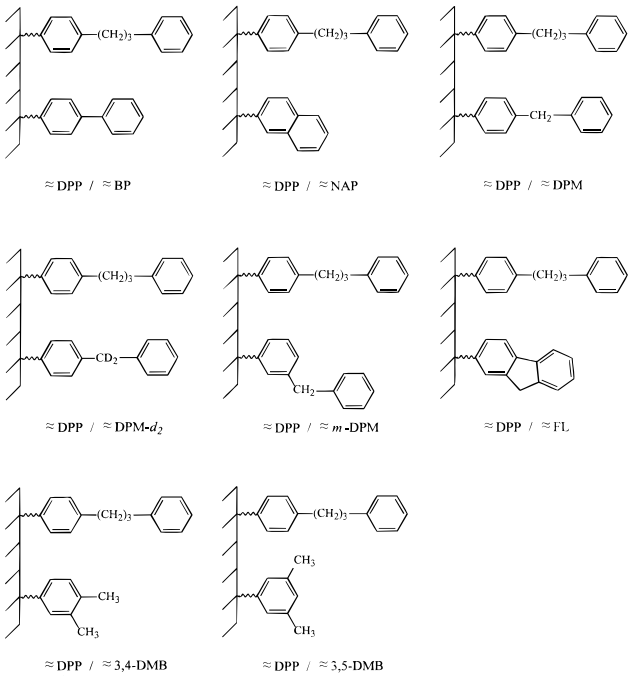

Figure 1. Silica-immobilized substrates that were synthesized and subjected to thermolysis at 375 °C.

hydroxydiphenylpropane (HODPP) with the silica hydroxyl groups did not occur with equal efficiencies, a fact that has been noted previously in the formation of two-component, self-assembled monolayers on gold surfaces.[12] As shown in Table 1, generally a larger ratio of spacer phenol to HODPP was required to obtain the desired final composition. The synthesis of the ≈DPP/≈FL surface was the notable exception. The reason for this finding is unknown, but was reproducible in repeat preparations. In one case, ≈DPP/≈BP, the attachment reaction was conducted in two serial steps. First, a saturated surface coverage of ≈BP was prepared. In the second step, diphenylpropane moieties were exchanged onto the surface replacing some of the ≈BP as shown in eq 3. This chemical

$$\approx BP + HODPP \rightleftarrows \approx DPP + HOBP \quad (3)$$

derivatization sequence is analogous to the serial derivatization of silica hydroxyl groups with two different alcohols via exchange.[13] No difference in the thermolysis behavior of ≈DPP/≈BP could be discerned for the one-step and two-step methods.

It has been reported that the methoxylation of a related fumed silica of comparable surface area, Aerosil, produces a maximum surface coverage of 2.9 ± 0.4 methoxy groups per nm^2 (corresponding to 0.96 mmol g^{-1}), and that this saturation surface coverage diminishes for bulkier alcohols.[13] Our previous analysis of the maximum surface coverages obtainable for *para*-substituted phenyl derivatives based on molecular size, using low-index surfaces of crystalline silicas as idealized models, predicted values in the range of 1.5−2.0 molecules nm^{-2} if serious steric interference is to be avoided.[6] This result has been substantiated for several examples.[6] The combined surface coverages shown in Table 1 generally fall within this range with only the dimethylbenzene spacer surfaces falling somewhat short of this range. This may be a consequence of the higher volatility of the precursor phenols compared with the other spacers

(11) (a) Poutsma, M. L.; Dyer, C. W. *J. Org. Chem.* **1982**, *47*, 4903. (b) Gilbert, K. E.; Gajewski, J. J. *J. Org. Chem.* **1982**, *47*, 4899. (c) Sweeting, J. W.; Wilshire, J. F. *Aust. J. Chem.* **1962**, *15*, 89. (d) King, H.-H.; Stock, L. M. *Fuel* **1982**, *61*, 1172.

(12) (a) Bain, C.; Whitesides, G. M. *Science* **1988**, *240*, 62. (b) Bain, C. D.; Whitesides. G. M. *J. Am. Chem. Soc.* **1988**, *110*, 3665.

(13) Zaborski, M.; Vidal, A.; Ligner, G.; Balard, H.; Papirer, E.; Burneau, A. *Langmuir* **1989**, *5*, 447.

Table 1. Composition of Two-Component Silica-Immobilized Substrates Synthesized

surface composition	surface coverages (mmol g^{-1})[a]	initial ratio (mol/mol)[b]	final ratio (mol/mol)[c]	total coverage (molecules nm^{-2})[d]	purity (%)
≈DPP/≈BP	0.13/0.51	e	3.9	2.2	99.9
	0.10/0.51	11.6	5.1	2.1	99.5
≈DPP/≈NAP	0.12/0.44	11.3	3.7	1.8	99.8
≈DPP/≈DPM	0.14/0.41	6.9	2.9	1.8	99.6
	0.13/0.36	6.9	2.8	1.7	99.7
≈DPP/≈DPM-d_2	0.12/0.35	6.9	2.9	1.6	99.7
	0.10/0.35	7.0	3.5	1.5	99.7
≈DPP/≈*m*-DPM	0.17/0.31	4.3	1.8	1.6	99.3
≈DPP/≈3,5-DMB	0.16/0.20	7.2	1.3	1.1	99.5
≈DPP/≈3,4-DMB	0.12/0.25	9.2	2.1	1.2	99.6
≈DPP/≈FL	0.17/0.42	1.7	2.5	2.0	99.3

[a] Surface coverage of each component on a per gram of derivatized silica basis. [b] Precursor spacer phenol to HODPP. [c] Surface-attached spacer to surface-attached DPP. [d] Based on surface area of 200 ± 25 m^2 g^{-1}. [e] Prepared by serial attachment rather than coattachment of the phenols, see text.

Table 2. Product Relationships from thermolysis ≈$Ph(CH_2)_3Ph$ in the Presence of Spacer Molecules[a]

surface composition	surface coverages (mmol g^{-1})	≈DPP conv range (%)[b]	≈DPP mass balance (%)	$C_8/{\approx}C_7$[c]	$C_7/{\approx}C_8$[d]	*S*[e]
≈DPP/≈BP	0.13/0.51	4.0−10.1	99 ± 3	1.11 ± 0.07	1.06 ± 0.09	1.09 ± 0.02
	0.10/0.51	3.3−7.2	100 ± 5	1.05 ± 0.12	0.99 ± 0.09	1.14 ± 0.04
≈DPP/≈NAP	0.12/0.44	2.2−7.0	95 ± 2	1.02 ± 0.06	1.01 ± 0.03	1.08 ± 0.02
≈DPP/≈DPM	0.14/0.41	3.9−13.8	98 ± 1	1.04 ± 0.05	1.11 ± 0.11	0.91 ± 0.03
	0.13/0.36	2.4−14.1	94 ± 3	1.01 ± 0.06	1.10 ± 0.06	0.91 ± 0.02
≈DPP/≈DPM-d_2	0.12/0.35	1.3−11.9	96 ± 5	0.99 ± 0.06	1.13 ± 0.11	0.99 ± 0.02
	0.10/0.35	2.0−15.2	101 ± 3	0.98 ± 0.07	1.07 ± 0.07	0.97 ± 0.03
≈DPP/≈*m*-DPM	0.17/0.31	1.9−9.7	94 ± 3	0.96 ± 0.03	1.01 ± 0.05	0.94 ± 0.02
≈DPP/≈3,5-DMB	0.16/0.20	3.5−6.8	100 ± 1	1.03 ± 0.04	1.09 ± 0.06	1.10 ± 0.03
≈DPP/≈3,4-DMB	0.12/0.25	1.5−4.6	97 ± 4	1.05 ± 0.05	1.07 ± 0.07	1.08 ± 0.01
≈DPP/≈FL	0.17/0.42	2.6−14.8	99 ± 1	0.95 ± 0.04	1.58 ± 0.19[f]	0.88 ± 0.01

[a] All thermolyses performed at 375 °C. [b] Number of thermolyses in conversion range was 4−9. [c] Product ratio, $PhCH{=}CH_2/{\approx}PhCH_3$. [d] Product ratio, $PhCH_3/({\approx}PhCH{=}CH_2 + {\approx}PhCH_2CH_3)$. [e] Thermolysis selectivity defined by yield ratio, $PhCH{=}CH_2/PhCH_3$. For thermolysis of ≈DPP without spacers at surface coverages of 0.59, 0.14, and 0.10 mmol g^{-1}, *S*-values of 0.96, 1.09, and 1.21, respectively, were obtained.[10] [f] Surface-attached styrene reacted with spacer, see text.

studied, which we have recently found results in poorer attachment efficiencies,[14] and the increased steric requirements of the *m*-methyl groups.

Thermolysis Products. Thermolyses were conducted at 375 °C under vacuum in sealed tubes. The experiment is designed such that volatile products are continuously removed from the heated zone during the reaction and are collected in a cold trap for analysis. Also collected are small quantities (3−8%) of unreacted parent phenols that are produced by a condensation reaction with residual adjacent surface silanol groups (to form the phenols and a siloxane linkage) in a process analogous to the dehydroxylation of silica itself at these elevated temperatures.[15] Silica-attached products are analyzed after completion of the reaction by means of a base hydrolysis procedure. Thermolysis of ≈DPP produces two pairs of cracking products shown in eq 4 in nearly equal amounts.[9a] Thermolysis of the

$$\approx Ph(CH_2)_3PH \rightarrow PhCH_3 + {\approx}PhCH{=}CH_2 + {\approx}PhCH_3 + PhCH{=}CH_2 \quad (4)$$

two-component surfaces containing ≈DPP likewise produces these compounds as the major products (>98−99%). Small quantities (0.3−2.0%) of $\approx PhCH_2CH_3$ are also observed as well as occasional trace amounts (<0.1%) of $PhCH_2CH_3$ and $PhCH_2$-CH_2Ph. No new products are detected in the presence of the coattached spacer molecules except in the case of ≈DPP/≈FL (*vide infra*).

Mass and stoichiometric balances are shown in Table 2 for an average of 4−9 thermolyses for each two-component surface. The fragment balances are defined as $C_8/{\approx}C_7$ [for $PhCH{=}CH_2/{\approx}PhCH_3$] and $C_7/{\approx}C_8$ [for $PhCH_3/({\approx}PhCH{=}CH_2 + {\approx}PhCH_2$-$CH_3)$]. As seen from Table 2, these balances are close to the ideal value of unity as required by stoichiometry, and as observed previously for surfaces containing only ≈DPP.[9a] The only exception is for the ≈DPP/≈FL sample, where the $\approx PhCH{=}CH_2$ product yield decreases with increasing ≈DPP conversion. This is accompanied by the formation of increasing quantities of two new isomeric products that account for 3−9% of the total products. These products have not been completely characterized, but GC-MS data (see Experimental Section) indicate that the major isomer (75%) results from the addition of surface-attached fluorenyl radicals to the surface-attached styrene. Hence, the excellent mass and stoichiometric balances exhibited in Table 2 provide confidence in the quantitation, and that all significant products have been identified. There is little regioselectivity in the thermal cracking of ≈DPP as illustrated in the last column of Table 2. This selectivity is monitored by the $PhCH{=}CH_2/PhCH_3$ yield, and its origin will be discussed below.

Reaction Rates. The initial reaction rates for ≈DPP at 375 °C in the presence of the spacer molecules were obtained from the slopes of linear regressions of ≈DPP conversion versus reaction time with reaction extents limited to <15%. Several examples of these data and the associated linear regression plots are shown in Figure 2. The regression lines typically extrapolate to slightly positive conversions at zero time, suggestive that there is a faster rate component for the very early stages of the reaction. The origin of this effect for the long-chain, free-radical decomposition of ≈DPP, which was observed previously for single-component surfaces of ≈DPP,[9a] is not known. However, the rate disturbance affects only the very earliest stage of the

(14) A similar low surface coverage was obtained for the attachment of phenol to the silica surface.[7]

(15) Iler, R. K. *The Chemistry of Silica*; Wiley: New York, 1979.

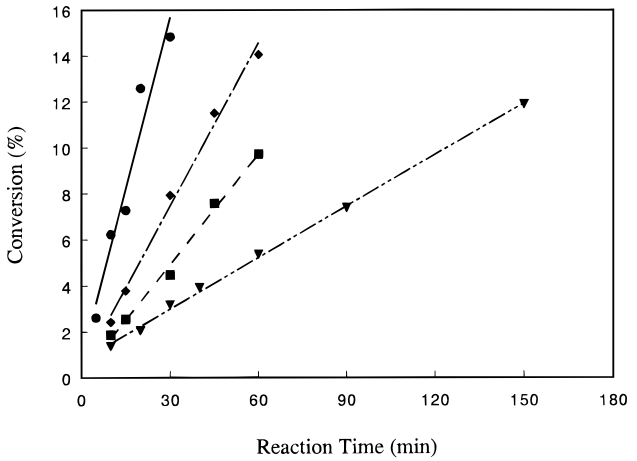

Figure 2. Examples of measurement of initial reaction rates for ≈DPP thermolysis at 375 °C: (●) ≈DPP/≈FL, (◆) ≈DPP/≈DPM, (■) ≈DPP/≈*m*-DPM, (▼) ≈DPP/≈DPM-d_2.

reaction and is substantially over by ca. 1% conversion. The reaction rates, their associated errors, and the correlation coefficients for the linear regressions are collected in Table 3.

Discussion

Rate and Selectivity in ≈DPP Thermolysis. If the rate of decomposition of 1,3−diphenylpropane were governed solely by homolysis of its weakest bond (ca. 74 kcal mol^{-1}) to form $PhCH_2^{\bullet}$ and $PhCH_2CH_3^{\bullet}$, then DPP would be stable at 400 °C with a half-life on the order of 19 years.[16] The fact that DPP is thermally reactive at 375 °C derives from the incursion of a long kinetic chain, free-radical process that also occurs readily for the silica-immobilized form.[9a] The free-radical chain decomposition mechanism has been discussed in detail elsewhere,[9a,11] and only the key features will be reproduced here.

The thermal cracking of ≈DPP produces the products shown in eq 4 by a radical chain process that is initiated by a very small amount of C−C homolysis (to form $\approx PhCH_2^{\bullet}$ and $PhCH_2$-$CH_2^{\bullet}$, or $PhCH_2^{\bullet}$ and $\approx PhCH_2CH_2^{\bullet}$). Kinetic chain lengths for the reaction, which can be accelerated by the addition of free-radical initiators, are estimated to be >250. The key chain propagation steps are shown in eqs 5−8. Chain termination

$$PhCH_2^{\bullet} + \approx Ph(CH_2)_3Ph \rightarrow PhCH_3 + \approx PhCH^{\bullet}CH_2CH_2Ph \text{ or } \approx PhCH_2CH_2CH^{\bullet}Ph \quad (5)$$
(**1**) (**2**)

$$\approx PhCH_2^{\bullet} + \approx Ph(CH_2)_3Ph \rightarrow \approx PhCH_3 + \mathbf{1} \text{ or } \mathbf{2} \quad (6)$$

$$\mathbf{1} \rightarrow \approx PhCH{=}CH_2 + PhCH_2^{\bullet} \quad (7)$$

$$\mathbf{2} \rightarrow \approx PhCH_2^{\bullet} + PhCH{=}CH_2 \quad (8)$$

occurs through coupling of benzyl radicals. The overall rate of decomposition of ≈DPP is governed by the rates of the hydrogen transfer steps (eqs 5 and 6) to produce benzylic radicals **1** and **2**, which can then undergo rapid unimolecular β-scission (eqs 7 and 8). At a saturation surface coverage of 0.59 mmol g^{-1}, ≈DPP thermally decomposes readily at 375 °C with an initial rate of conversion of [24 (±4) × 10^{-4}]% s^{-1}.[9a] This rate is comparable to that measured for liquid-phase DPP at 375 °C.[11a,b] The rate of decomposition of DPP in both silica-immobilized and fluid-phase forms decreases dramatically with decreases in surface coverage and concentration, respectively, as the rate of the bimolecular hydrogen atom transfer steps decrease. For ≈DPP, a decrease in surface coverage to 0.14 and 0.10 mmol g^{-1} results in a 22- and 33-fold decrease in rate, respectively.[9a] Hydrogen transfer step 6 might be expected to be particularly sensitive to surface coverage decreases as the spatial separation between these two reactants on the surface increases as depicted below.

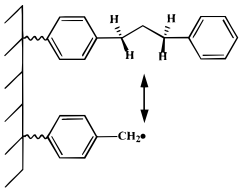

This surface coverage effect also results in a subtle shift in regioselectivity (*S*) in the reaction, which depends on the relative rates of production of the benzylic radicals, **1** and **2**, in eqs 5 and 6 and is monitored by the $PhCH{=}CH_2/PhCH_3$ yield ratio. As shown previously, *S*-values of 0.96, 1.09, and 1.21 are obtained at ≈DPP surface coverages of 0.59, 0.14, and 0.10 mmol g^{-1}, respectively.[9a,10] At high surface coverage, the *S*-value of 0.96 reflects the very slight preference for formation of **1** as a consequence of a small substituent effect from the *p*-silyloxy substituent, and is comparable to that measured for fluid-phase *p*-$Me_3SiOPh(CH_2)_3Ph$.[9a] The increase in *S* with decreasing surface coverage indicates an increasing preference for generating the less stabilized benzylic radical, **2**. This observation has been interpreted as resulting from restricted diffusion which leads to a small increasing preference for abstraction of the benzylic hydrogen farthest from the surface as the ≈DPP molecules and $\approx PhCH_2^{\bullet}$ become increasingly separated.

Spacer molecules are anticipated to have an impact on the hydrogen transfer steps and, thus, on the rates and selectivities in the ≈DPP thermolysis. As can be seen in Table 3, the rate of ≈DPP thermolysis is extremely sensitive to the structure of the spacer molecule. Only a small impact on product selectivity (Table 2) is detected. A more detailed analysis of the impact of the spacer molecules will now be discussed.

Effect of Biphenyl and Naphthalene Spacers. The aromatic spacer molecules ≈BP and ≈NAP are thermally stable at 375 °C, and no new products were detected from the thermolysis of ≈DPP in the presence of these spacers. The rate of ≈DPP thermolysis (ca. (2 × 10^{-4})% s^{-1}) is very similar to that for surfaces containing only ≈DPP at similar low ≈DPP surface coverages. In addition, the selectivity values of 1.08−1.14 are also of similar size to those measured for ≈DPP alone at similar surface coverages. Hence, it appears that dilution of ≈DPP surfaces with these inert aromatic spacers has little impact on the thermolysis behavior, and is similar to dilution with "empty space".

We have examined two different methods for preparation of batches of the ≈DPP/≈BP material to see if there is any effect of the surface derivatization method on thermolysis behavior. In addition to the conventional one-step preparation, where both components were attached in a single step, a serial two-step method for attachment was also employed. In this latter case, a saturation surface coverage of ≈BP (ca. 0.6 mmol g^{-1}) was prepared, and then DPP moieties exchanged onto the surface in a second step as shown in eq 3. As can be seen from the thermolysis data (Tables 2 and 3), no difference in the rate or product selectivity could be discerned between these two methods of preparation.

(16) Poutsma, M. L. *Energy Fuels* **1990**, *4*, 113.

Table 3. Thermolysis Rates for ≈Ph$(CH_2)_3$Ph at 375 °C: Impact of Spacer Molecules

surface composition	surface coverages (mmol g^{-1})	no. of thermolyses	rate × 10^4 (% s^{-1})[a]	corr coeff, r[b]
≈DPP[c]	0.14[d]	7	1.1 (±0.2)	0.955
	0.10[e]	4	0.72 (±0.05)	0.997
≈DPP/≈BP	0.13/0.51[f]	4	2.2 (±0.5)	0.955
	0.10/0.51	4	2.4 (±0.8)	0.946
≈DPP/≈NAP	0.12/0.44	6	1.9 (±0.2)	0.977
≈DPP/≈DPM	0.14/0.41	4	37 (±2.4)	0.996
	0.13/0.36	5	39 (±2.1)	0.997
≈DPP/≈DPM-d_2	0.12/0.35	9	13 (±0.4)	0.997
	0.10/0.35	7	15 (±0.9)	0.992
≈DPP/≈*m*-DPM	0.17/0.31	5	27 (±1.2)	0.997
≈DPP/≈3,5-DMB	0.16/0.20	5	7.1 (±1.1)	0.967
≈DPP/≈3,4-DMB	0.12/0.25	5	8.5 (±1.6)	0.951
≈DPP/≈FL	0.17/0.42	5	83 (±12)	0.970

[a] Initial rates determined from the slopes of linear regressions of ≈DPP conversion versus reaction time with reaction extents limited to <15%. [b] Correlation coefficient, r, from linear regression analysis. [c] ≈DPP surface with no spacer molecules. At a ≈DPP saturation surface coverage of 0.59 mmol g^{-1}, a rate of 24 (±4) × 10^{-4} % s^{-1} was obtained[9a]. [d] From ref 9a. [e] From ref 10. [f] Prepared by serial attachment rather than coattachment of phenolic precursors, see text.

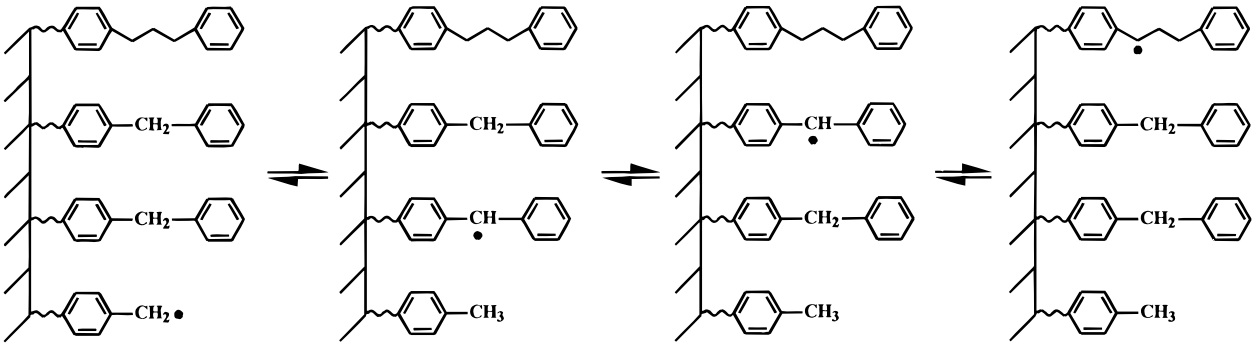

Figure 3. Hydrogen transfer, radical relay pathway under conditions of restricted diffusion.

In related studies on the preparation of self-assembled monolayers for mixtures of thiol molecules on gold surfaces,[12] the surface composition and structure of the resulting two-component, chemically modified surfaces are reported to be controlled principally by thermodynamics. Segregation of the components into islands is not observed. Even in cases where polar tail groups were present (such as alcohols), as well as long aliphatic chains (>C_{10}) where considerable interchain attractive van der Waals forces exist, no evidence for segregation was found.[12] In our study, where only short aliphatic chains and nonpolar tail groups are emanating from the surface, formation of well-dispersed surfaces, whose composition is most likely controlled by the thermodynamics of the surface modification, is similarly expected.

Effect of Diphenylmethane Spacers. Thermolysis of ≈DPP/≈DPM surfaces produces the standard slate of products with no new products observed from the thermally stable ≈DPM spacer. However, in contrast to the inert aromatic spacers described above, the presence of coattached diphenylmethane moieties has a dramatic effect on the rate of ≈DPP thermolysis as well as altering the regioselectivity value, S. The ≈DPP thermolysis rate (Table 3) is accelerated by a factor of 38 compared with ≈DPP alone at a corresponding surface coverage of 0.14 mmol g^{-1}, and a factor of ca. 16−20 compared with the ≈BP and ≈NAP spacers.[17] This behavior of the DPM spacer is specific to surface immobilization, since in related fluid-phase studies DPM behaved like other inert diluents.[11a,b] Furthermore, in the presence of ≈DPM, the regioselectivity (Table 2) is reduced to a value of 0.91 from values in the range of 1.08−1.14 in the presence of ≈BP and ≈NAP spacers. This lower value for S is more typical of saturated coverages of single-component surfaces of ≈DPP.

A possible explanation of these results is that rapid hydrogen transfer steps involving ≈DPM are occurring that allow radical centers to be shuttled across the surface until radicals **1** or **2** are formed that undergo β-scission. This proposed hydrogen transfer, radical relay process, which would alleviate some of the diffusional constraints, is illustrated in Figure 3 for the chain-carrying, surface-attached benzyl radical and for production of radical **1**. The result of such a process would be to increase the rate of the hydrogen transfer propagation steps (particularly eq 6) for the ≈DPP reaction by decreasing the effective distance between a ≈DPP molecule and radical centers on the surface. The values of S < 1.0 for ≈DPP/≈DPM surfaces are also consistent with this premise of a reduced separation between ≈DPP molecules and radical centers on the surface. The radical relay phenomenon illustrated in Figure 3 would effectively eliminate the distance-dependent conformational constraints on the hydrogen abstraction reactions from ≈DPP that resulted in the unexpected change in regioselectivity at low surface coverages of ≈DPP alone (favoring formation of **2** over **1**), and which is also observed for ≈DPP in the presence of the aromatic spacer molecules that do not contain reactive benzylic hydrogens to participate in the relay process.

As shown from the data in Tables 2 and 3, the use of the isomeric *m*-diphenylmethane spacer molecule similarly produces enhanced rates of decomposition for ≈DPP and S < 1.0. The rate enhancement is not quite as large as the *para* analog, perhaps as a consequence of orientation effects on the surface. However, the ≈m-DPM spacer is still clearly effective at participating in the radical relay process and contributing to

(17) The rates presented for ≈DPP/≈DPM surfaces are recently measured, and are a factor of ca. 1.8 larger than those reported in the earlier communication.[10]

enhanced rates for ≈DPP decomposition compared with the inert spacer molecules.

To gain additional evidence for the involvement of ≈DPM in the novel radical relay process depicted in Figure 3, thermolysis studies of ≈DPP/≈DPM-d_2 were conducted where the deuterium is located at the active methylene position as shown in Figure 1. GC-MS analysis of ≈DPP/≈DPM-d_2 reactions conducted at <5% conversion gave a deuterium distribution in the vapor-phase toluene product of 50% $PhCH_3$ and 50% $PhCH_2D$. GC-MS analysis (see Experimental Section) of the surface-attached toluene product, following liberation from the surface as cresol and derivatization to the trimethylsilyl ether, gave the composition 39% ≈$PhCH_3$, 51% ≈$PhCH_2D$, and 10% ≈$PhCHD_2$. No deuterium incorporation could be measured in the $PhCH{=}CH_2$ and ≈$PhCH{=}CH_2$ products. The results provide direct evidence for the involvement of D (H) transfer between ≈DPM-d_2 (-h_2) and both chain-carrying vapor-phase and surface-attached benzyl radicals. The formation of ≈$PhCHD_2$ suggests that the surface-attached toluene product can also participate in the hydrogen transfer, radical relay process to some extent. This observation is supported by studies of dimethylbenzene spacer molecules described later. If the hydrogen transfer, radical relay process described above is the key reason for the enhanced thermolysis rates for ≈DPP in the presence of ≈DPM spacers, then one would expect to observe a kinetic isotope effect for the ≈DPP/≈DPM-d_2 case. From a comparison of the rate data at 375 °C for ≈DPP/≈DPM-h_2 and ≈DPP/≈DPM-d_2 in Table 3, a kinetic isotope effect of 2.7 ± 0.2 can be calculated. In the absence of tunneling, the maximum deuterium kinetic isotope effect, k_H/k_D, for hydrogen transfer between carbon centers based on the zero-point energy difference for the C−H stretching mode is 2.4 at 375 °C.[18] However, large isotope effects in excess of the classical limits have been measured for hydrogen abstraction by benzyl[19] and 2-allylbenzyl[18] radicals at 160−170 °C, and the involvement of tunneling effects on these H-atom transfers has been demonstrated. An example relevant to the current work is H abstraction from diphenylmethane, for which isotope effects of 6.6 at 160 °C (2-allylbenzyl radical)[18] and 7.1 at 170 °C (benzyl radical)[19] have been reported. Hence, as a consequence of the involvement of tunneling in the H transfer between benzylic sites, extrapolation of these isotope effect values to higher temperatures is uncertain. However, an isotope effect of at least 3 at 420 °C has been invoked to explain the H(D) incorporation selectivity in the toluene product from thermolysis of $PhCD_2CH_2Ph$ under nitrogen.[20] Furthermore, in our recent study of the thermolysis of liquid-phase $PhCD_2CH_2OPh$, a kinetic isotope effect of 2.6 at 375 °C was observed compared to the protium analog.[21] Hence, the measured isotope effect of 2.7 at 375 °C for the thermolysis of ≈DPP in the presence of ≈DPM-h_2 (d_2) is consistent with the proposed radical relay process in which H-atom transfers from the DPM spacer molecules play a key role in controlling the rate of ≈DPP thermolysis.

The amount of deuterium incorporation in the vapor-phase toluene product generated from thermolysis of ≈DPP/≈DPM-d_2 at a surface coverage of 0.12/0.35 mmol g^{-1} is also consistent with available kinetic data. The vapor-phase benzyl radicals competitively abstract H from ≈DPP (eq 9) or D from ≈DPM-d_2 (eq 10), respectively, giving a measured $PhCH_3/PhCH_2D$

$$PhCH_2^{\bullet} + \approx Ph(CH_2)_3Ph \rightarrow PhCH_3 + \mathbf{1} \text{ or } \mathbf{2} \qquad (9)$$

$$PhCH_2^{\bullet} + \approx PhCD_2Ph \rightarrow PhCH_2D + \approx PhCD^{\bullet}Ph \qquad (10)$$

product ratio of 1.0. This value along with the ≈DPM-d_2/≈DPP surface coverage ratio of 2.9 leads to $k_{\approx DPP}/k_{\approx DPM\text{-}d_2} = 1.4$ for H(D) abstraction on a per active H(D) basis. The relative rate for hydrogen abstraction by $PhCH_2^{\bullet}$ from DPM-h_2 versus DPP has been measured as 3.3 (per active hydrogen basis) at 170 °C.[22] Extrapolation of this value to 375 °C and making the reasonable assumption that surface immobilization will not have any significant effect gives $k_{\approx DPM\text{-}h_2}/k_{\approx DPP} = 2.2$. Hence, a kinetic isotope effect of $k_{\approx DPM\text{-}h_2}/k_{\approx DPM\text{-}d_2} = 1.4 \times 2.2 = 3.1$ at 375 °C would be required to give the observed $PhCH_3/PhCH_2D$ product ratio, which is consistent with the data presented above.

What is the origin of the efficacy of the radical relay process observed for the ≈DPP/≈DPM system illustrated in Figure 3? Our current hypothesis centers around the fact that bimolecular hydrogen transfer steps are occurring between reactants that are constrained to the surface and are, therefore, preorganized for reaction. This preorganization can be considered as resulting in a "reduction in the dimensionality of the reaction space", which has been proposed to contribute to enhanced rates of reactions on the surfaces of layered solids such as clays.[23,24] Enhanced rates for bimolecular reactions under such conditions then result from enhanced encounter rates. An implication of this argument is that solid support surfaces with fractal dimension, D, of ca. 2 should be more likely to exhibit this kinetic enhancement effect than porous solids with D-values near 3.[23] The fractal dimension for a nonporous, fumed silica support, Aerosil 200, analogous to the one employed in this work has been measured to be 2.08 and is consistent with the argument presented above.[25]

Therefore, the pyrolysis mechanism of ≈DPP in the presence of ≈DPM must be augmented by the inclusion of the additional propagation steps 11−13 shown below. In this process, the

$$PhCH_2^{\bullet} \text{ (or } \approx PhCH_2^{\bullet}) + \approx PhCH_2Ph \rightarrow PhCH_3 \text{ (or } \approx PhCH_3) + \approx PhCH^{\bullet}Ph \qquad (11)$$

$$\approx PhCH^{\bullet}Ph + \approx PhCH_2Ph \rightarrow \approx PhCH_2Ph + \approx PhCH^{\bullet}Ph \qquad (12)$$

$$\approx PhCH^{\bullet}Ph + \approx Ph(CH_2)_3Ph \rightarrow \approx PhCH_2Ph + \mathbf{1} \text{ or } \mathbf{2} \qquad (13)$$

diphenylmethane molecules serve as catalysts for translocating radical centers across the surface by a hydrogen transfer process that does not involve conventional diffusion. A related phenomenon, termed "hydrogen or radical hopping", has been invoked to explain the radiation-induced chemistry of certain polymers.[26] For example, Clough has reported that the γ irradiation at room temperature of a cocrystallized mixture of $C_{24}H_{50}$ and $C_{24}D_{50}$ resulted in extensive isotopic exchange in the solid state that was not observed for a similar isotropic mixture irradiated in the liquid phase.[26] Hence, this type of

(18) Franz, J. A.; Alnajjar, M. S.; Barrows, R. D.; Kaisaki, D. L.; Camaioni, D. M.; Suleman, N. K. *J. Org. Chem.* **1986**, *51*, 1446.
(19) Bockrath, B. C.; Bittner, E. W.; Marecic, T. C. *J. Org. Chem.* **1986**, *51*, 15.
(20) (a) Guthrie, R. D.; Shi, B.; Rajagopal, V.; Ramakrishnan, S.; Davis, B. H. *J. Org. Chem.* **1984**, *59*, 7426. (b) Rajagopal, V.; Guthrie, R. D.; Shi, B.; Davis, B. H. *Prepr. Pap.-Am. Chem. Soc. Div. Fuel Chem.* **1993**, *38*, 1114.
(21) Britt, P. F.; Buchanan, A. C., III; Malcolm, E. A. *J. Org. Chem.* **1995**, *60*, 6523.
(22) Bockrath, B.; Bittner, E.; McGrew, J. *J. Am. Chem. Soc.* **1984**, *106*, 135.
(23) Laszlo, P. *Acc. Chem. Res.* **1986**, *19*, 121.
(24) For a recent theoretical analysis of the effect of reduction in dimensionality on bimolecular reaction rates for interfacial reactions, see: Mandeville, J. B.; Kozak, J. J. *J. Am. Chem. Soc.* **1992**, *114*, 6139.
(25) Pines-Rojanski, D.; Huppert, D.; Avnir, D. *Chem. Phys. Lett.* **1987**, *139*, 109.
(26) Clough, R. L. *J. Chem. Phys.* **1987**, *87*, 1588 and references therein.

hydrogen transfer, radical migration mechanism may have broader involvement in the chemistry of radicals in the solid state. In the next section, we investigate how this process is affected by the nature of the hydrogen donating spacer molecule.

Effect of Dimethylbenzene and Fluorene Spacers. It seemed likely that the radical relay process described above for ≈DPM spacers would also occur for other spacer molecules that contain benzylic C−H bonds. However, the rate of decomposition of ≈DPP could depend to some degree on the kinetics of hydrogen transfer from the spacer molecule to chain-carrying benzyl radicals. In addition, the kinetics of H transfer may also include a contribution from molecular orientation of the spacer as witnessed by the ≈*p*-DPM and ≈*m*-DPM comparison shown above. ≈DMB and ≈FL were chosen as spacer molecules since the rate constants for H transfer to benzyl radicals should bracket the ≈DPM spacer. In fluid phases, the relative rates of hydrogen abstraction by benzylic radicals are approximately inversely correlated with C−H bond strengths.[16] The rate constants (k, M^{-1} s^{-1}; per active hydrogen) at 160 °C for H abstraction by *o*-allylbenzyl have been reported from 1,3-dimethylbenzene (2.20), diphenylmethane (40.5), and fluorene (520).[18] These rate differences for H abstraction should be attenuated at higher temperatures. Using the Arrhenius parameters presented in ref 18 and extrapolation to 375 °C, the relative rate constants for 1,3-dimethylbenzene, diphenylmethane, and fluorene of 1.0, 7.4, and 82, respectively, can be estimated. The large increase in rate going from diphenylmethane to fluorene is principally a consequence of the fact that the cyclic fluorene molecule does not require phenyl bond rotations to be frozen out in the transition state for the H transfer. However, in the surface-attached analog, the fact that the hydrogens are attached to a carbon locked in a ring could potentially lead to geometrical constraints in the hydrogen transfer steps on the surface and substantially modify the potential rate enhancement.

As observed from the data in Table 3, the rate of thermolysis of ≈DPP at 375 °C indeed depends on the structure of the hydrogen donor spacer, increasing in the order ≈DMB < ≈DPM < ≈FL. The relative rates for ≈DPP thermolysis in the presence of the ≈3,5-DMB, ≈*m*-DPM, and ≈FL spacers (all with *meta* linkages relative to the active benzylic hydrogens, see Figure 1) are 1.0, 3.8, and 11.7, respectively. If these rates are statistically corrected for the number of active hydrogens, the relative rates become 1.0, 11.4, and 35.1, respectively. This ordering correlates with the kinetics for H transfer to benzylic radicals in fluid phases described above, and provides additional support for the significance of these reaction steps in controlling the rates of ≈DPP thermolysis in the presence of spacer molecules.

Thermolysis of ≈DPP in the presence of ≈3,5-DMB and ≈3,4-DMB gave rates of (7.1×10^{-4} and 8.5×10^{-4})% s^{-1}, respectively. No new thermolysis products were detected in the presence of these spacers. The thermolysis rates are not significantly affected by the nature of the methyl-substitution pattern of the ≈DMB spacer. The rates are somewhat faster than for surfaces of ≈DPP alone at comparable surface coverages and ≈DPP surfaces with ≈BP or ≈NAP spacers, indicating that methylated benzenes can participate in the radical relay process to a limited extent. This observation also explains the formation of some dideuterated, surface-attached toluene, ≈$PhCHD_2$, in the thermolysis of ≈DPP/≈DPM-d_2 as described above. These results suggest that any molecule possessing benzylic hydrogens should be capable of participating in the radical relay process.

Thermolysis of ≈DPP in the presence of ≈FL produced the fastest rate for ≈DPP decomposition of all the spacer molecules investigated. However, the reaction is complicated by the fact that the fluorene spacer does not serve solely as a radical relay catalyst, and actually becomes involved in product formation. GC-MS analysis (see Experimental Section) suggests that new product formation arises from addition of the surface-attached fluoren-9-yl radical intermediate (≈FL•) to the surface-attached styrene product in a chain transfer step (eq 14).[27] This process was not observed for the structurally related ≈*m*-DPM spacer. The difference is likely a consequence of the less sterically congested radical center in the cyclic fluorenyl radical intermediate, which has significant impact on the kinetics of radical additions to alkenes.[27] Interestingly, the sole reaction pathway observed for the resulting adduct radical is hydrogen abstraction from ≈DPP (eq 15) or ≈FL (eq 16). This process provides an additional pathway for radical centers to be relayed across the surface that can apparently contribute to the facile decomposition of ≈DPP.

$$\approx FL^{\bullet} + \approx PhCH{=}CH_2 \rightarrow \approx PhCH^{\bullet}CH_2{-}FL\approx \quad (14)$$

$$\approx PhCH^{\bullet}CH_2{-}FL\approx + \approx Ph(CH_2)_3Ph \rightarrow \approx PhCH_2CH_2{-}FL\approx + \mathbf{1} + \mathbf{2} \quad (15)$$

$$\approx PhCH^{\bullet}CH_2{-}FL\approx + \approx FL{-}H \rightarrow \approx PhCH_2CH_2{-}FL\approx + \approx FL^{\bullet} \quad (16)$$

Summary and Implications for Fuel Processing. This study has demonstrated that the rate of thermal cracking of surface-immobilized 1,3-diphenylpropane at 375 °C can span a substantial range that is highly dependent on the structure of neighboring molecules on the surface. Neighboring molecules that possess benzylic hydrogens are capable of participating in a series of rapid hydrogen transfer steps with free radical intermediates. The impact of this process is to provide a mechanism for radical centers to rapidly relocate in a diffusionally constrained environment without the need for physical movement. The consequence of this process in the current example is enhanced rates for the radical chain decomposition of ≈DPP compared with the presence of inert aromatic spacer molecules. The unexpected high efficiency of this process is currently attributed to the reduced dimensionality of the reaction space (higher encounter frequency) for these immobilized reactants on the smooth surface of the amorphous, nonporous silica particles. There may exist an optimum set of spacer chemical structures that possess the appropriate thermochemistry and geometry for hydrogen transfer to promote the radical relay phenomenon under conditions of restricted diffusion, and we continue to explore additional spacer molecules.

These results for free-radical reactions on chemically modified surfaces have significant implications for the thermochemical conversion of hydrogen deficient fuel resources such as coal into liquid fuels or higher value chemicals. Conversion of coal into desirable hydrogen rich products can be hampered by the cross-linked network structure and by substantial domains of microporosity. Access of hydrogen donor solvents to stabilize thermally generated radical sites, or cracking of refractory cross-links through generation of labile radicals by hydrogen abstraction (as typified by ≈DPP in the current investigation), can be

(27) Kinetics of radical additions to alkenes in fluid phases contain contributions from bond strength, polar, and steric effects.[28,29] Radical additions to styrene are well-known,[29] and are kinetically competitive with reverse dissociation at 375 °C.[21,9a]

(28) Fischer, H. In *Substituent Effects in Radical Chemistry*; Viehe, H. G., Janousek, Z., Merenyi, R., Eds.; D. Reidel: Dordrecht, 1986, Chapter 8.

(29) Giese, G. *Angew. Chem., Int. Ed. Engl.* **1983**, *22*, 753.

diffusionally limited. Our results in a diffusionally constrained model system suggest that some of these diffusional limitations may be overcome by a unique hydrogen transfer, radical relay mechanism. This discovery provides new insights into how the native network structure of coal may control hydrogen utilization during its thermal processing.

Experimental Section

GC analysis was performed on a Hewlett Packard 5890 Series II gas chromatograph employing a J & W Scientific 30 m × 0.25 mm DB^{-1} methylsilicone column (0.25 μm film thickness) and flame-ionization detection. Detector response factors were determined relative to cumene (hydrocarbon products) or 2,5-dimethylphenol and *p*-(2-phenylethyl)phenol (phenolic products) as internal standards as previously described.[9a] Mass spectra were obtained at 70 eV with a Hewlett Packard 5995A GC-MS or a Hewlett-Packard 5972A/5890 Series II GC-MS equipped with a capillay column matched to that used for GC analyses.

Materials. Benzene was distilled from lithium aluminum hydride before use. High-purity acetone, methylene chloride, and water were commercially available and used as received. Cumene was fractionally distilled (2×) and 2,5-dimethylphenol was recrystallized (3×) from hexanes prior to use. The synthesis and purification of *p*-$HOC_6H_4(CH_2)_3C_6H_5$ (HODPP)[9a] and *p*-$HOC_6H_4(CH_2)_2C_6H_56$ have been previously described. *p*-Phenylphenol, 2-hydroxynaphthalene, *p*-benzylphenol, 3,4-dimethylphenol, and 3,5-dimethylphenol were commercially available and were purified to >99.9%. *p*-Phenylphenol and *p*-benzylphenol were purified by repeated crystallizations from benzene/hexanes. 2-Naphthol was purified by recrystallization from ethanol/water followed by carbon tetrachloride and sublimation at 110 °C at 0.01 Torr. The dimethylphenol isomers were purified by chromatography on a silica gel column with benzene as eluant, followed by recrystallization from hexanes. *m*-Benzylphenol was synthesized as described previously[30] and purified to 99.6% by distillation at 135−140 °C at 0.25 Torr. The deuterated *p*-benzylphenol analog, *p*-$HOC_6H_4CD_2C_6H_5$, was synthesized in three steps from *p*-hydroxybenzophenone to give a product of 99.9% chemical purity and >95% isotopic purity (by GC-MS). The synthesis involved formation of the methyl ether derivative with potassium carbonate and methyl iodide in DMF, followed by reduction of the ketone with $LiAlD_4/AlCl_3$ in ether,[31] and subsequent demethylation with $(CH_3)_3SiCl$/NaI in refluxing acetonitrile.[32] 2-Hydroxyfluorene was synthesized by the Baeyer−Villeger oxidation of 2-fluorenecarboxaldehyde[33] and purified to 99.9% by repeated crystallizations from toluene.

Preparation of Surface-Attached Materials. Preparation of the two-component surfaces followed previously described methodologies for preparing single-component surfaces.[6,9] A general description will be presented, and the final surface coverages and purities are given in Table 1. Cabosil M-5 (Cabot Corp., 200 $m^2\ g^{-1}$, ca. 4.5 SiOH nm^{-2} or 1.5 mmol SiOH g^{-1}) was dried at 200 °C for 4 h. HODPP and the spacer phenol (2.25 combined equiv to 1.0 equiv of SiOH; ratio of phenols given in Table 1) were coadsorbed onto the silica by solvent evaporation of a benzene slurry. Surface attachment was performed in sealed, evacuated (10^{-5} Torr) Pyrex tubes at 225 °C for 1 h in a fluidized sand bath. Unattached phenols were sublimed from the sample by heating to 270 °C for 0.5−1.0 h at $5-10 \times 10^{-3}$ Torr. In the case of the ≈DPP/≈FL surface, an additional Soxhlet extraction with acetone was employed. Surface coverages were determined on 150−200 mg of surface-attached material by dissolution in 1 N NaOH overnight, addition of *p*-$HOC_6H_4(CH_2)_2C_6H_5$ (HOBB) as internal standard, acidification with HCl, extraction with CH_2Cl_2, drying over $MgSO_4$, solvent removal under reduced pressure, and silylation with *N,O*-bis(trimethylsilyl)trifluoroacetamide (BSTFA) in pyridine (2.5 M, 0.35 mL) to form the corresponding trimethylsilyl ethers. GC analysis of multiple assays provided surface coverages with reproducibility of ±3%.

Thermolysis Procedure. A weighed amount of sample (0.4−0.6 g) was placed in one end of a T-shaped Pyrex tube, evacuated, and sealed at ca. 2×10^{-6} Torr. The sample was inserted into a preheated temperature-controlled tube furnace (±1.0 °C) fitted with a copper sample holder, and the other end was placed in a liquid nitrogen bath. The volatile products collected in the trap were dissolved in acetone (0.1−0.3 mL) containing cumene as an internal standard and analyzed by GC and GC-MS. The small amounts of HODPP and spacer phenol that evolved into the trap were then analyzed by addition of HOBB in acetone as internal standard, evaporation of the solvent, silylation with BSTFA, and analysis by GC. The surface-attached products were analyzed by a base hydrolysis procedure analogous to that used for surface coverage assay except that 2,5-dimethylphenol was added as a GC internal standard in addition to HOBB. In this residue analysis, care must be taken to quickly extract the phenolic mixture away from the aqueous phase following acidification since the *p*-vinylphenol (corresponding to the ≈$PhCH{=}CH_2$ product) is unstable in the presence of acid.

Product Assignments. All products from thermolysis of ≈DPP have been previously identified.[9a] With the exception of the fluorene spacer, no additional products were detected in the two-component surfaces reported in this study. For the ≈DPP/≈FL thermolysis, two new isomeric products of composition $C_{21}H_{16}(OH)_2$ (M_r = 302) were identified by GC-MS, which added two trimethylsilyl groups upon silylation with BSTFA to give derivatives with M_r = 446. The mass spectrum (relative intensity) of the trimethylsilyl derivative of the major isomer (75%) is 446 (M^+, 2), 253 (10), 194 (31), 193 (100, $Me_3SiOC_6H_4CH_2CH_2$+), 73 (34), while that of the minor isomer is 446 (M^+, 22), 267 (33), 266 (10), 254 (21), 193 (17), 179 (20), 73 (100). The major isomer is tentatively assigned to the product resulting from the addition of the surface-attached fluoren-9-yl radical to the surface-attached styrene as shown in eqs 14−16.

Deuterium Distribution in ≈DPP/≈DPM-d_2 Thermolysis Products. The deuterium distribution in the thermolysis products was determined by GC-MS. Quantitative analysis of deuterium content in the vapor-phase toluene product employed known mixtures of $PhCH_3$ and $PhCH_2D$ for calibration standards, and accounted for contributions from $(M - H(D))^+$ fragment ions as well as ^{13}C isotopic contributions. Analysis of the deuterium content in $HOPhCH_3$ (from surface-attached toluene product) was based on the GC-MS analysis of the trimethylsilyl ether derivatives. Since there was no fragmentation to produce $(M - H)^+$ ions in $Me_3SiOPhCH_3$, parent ions at *m/e* 180 (-d_0), 181 (-d_1), and 182 (-d_2) were employed and corrected for ^{13}C and $^{29,30}Si$ isotopic contributions. Duplicate analyses agreed within ±4%.

Acknowledgment. This research was sponsored by the Division of Chemical Sciences, Office of Basic Energy Sciences, U.S. Department of Energy, under Contract No. DE-AC05-840R21400 with Lockheed Martin Energy Systems, Inc.

JA953548S

(30) McMillen, D. F.; Ogier, W. C.; Ross, D. S. *J. Org. Chem.* **1981**, *46*, 3322.
(31) Nystrom, R. F.; Berger, C. R. A. *J. Am. Chem. Soc.* **1958**, *80*, 2896.
(32) Olah, G. A.; Narang, S. C.; Gupta, B.; Malhotra, R. *J. Org. Chem.* **1979**, *44*, 1247.
(33) Godfrey, I. M.; Sargent, M. V.; Elix, J. A. *J. Chem. Soc., Perkin Trans. 1* **1974**, 1353.